OPEN ACCESS

University of BRISTOL

Peer reviewed version

Link to published version (if available):
10.1002/eqe.2694

Link to publication record in Explore Bristol Research
PDF-document

University of Bristol - Explore Bristol Research
General rights

SOIL-PILE-STRUCTURE INTERACTION: EXPERIMENTAL OUTCOMES FROM SHAKING TABLE TESTS

Maria Giovanna Durante, Luigi Di Sarno, George Mylonakis, Colin A Taylor, Armando Lucio Simonelli

Abstract

An effective way to study the complex seismic soil-structure interaction phenomena is to analyse the response of physical scaled models in 1-g or n-g laboratory devices. The outcomes of an extensive experimental campaign carried out on scaled models by means of the shaking table of the Bristol Laboratory for Advanced Dynamics Engineering (BLADE), University of Bristol, UK are discussed in the present paper. The experimental model comprises an oscillator connected to a single or a group of piles embedded in a bi-layer deposit. Different pile head conditions, i.e. free head and fixed head, several dynamic properties of the structure, including different masses at the top of the single degree of freedom system, excited by various input motions, e.g. white noise, sinedwells and natural earthquake strong motions recorded in Italy, have been tested. In the present work, the modal dynamic response of the soil-pile-structure system is assessed in terms of period elongation and system damping ratio. Furthermore, the effects of oscillator mass and pile head conditions on soil-pile response have been emphasized, when the harmonic input motions are considered.

Keywords: shaking table tests; soil-structure interaction; kinematic effects; inertial effects; period elongation; damping ratio

1. Introduction

The seismic response of piled foundations is a complex phenomenon, as it is affected by the movement of the surrounding soil which generates the so-called "kinematic" loading (Figure 1a), and the oscillations of the superstructure, which induces the so-called "inertial" loading (Figure 1b). The kinematic bending moments may be significant near the pile head, or for piles embedded in soils with high stiffness contrast between consecutive layers [1-6].
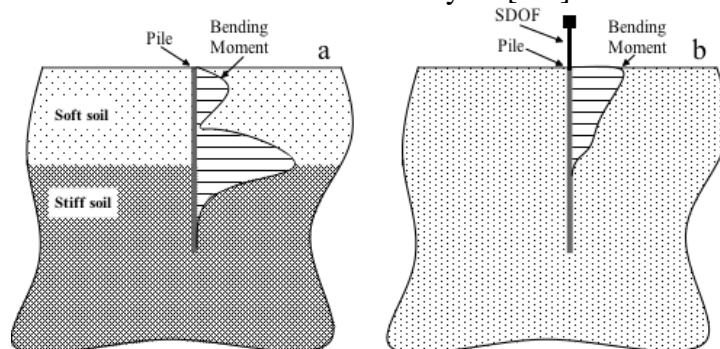

Figure 1. (a) kinematic and (b) inertial bending moments (qualitative patterns)

The reliable assessment of the dynamic behaviour of piled foundations under earthquake loading is of paramount importance for evaluating the seismic performance of flexibly-supported structures, especially when the foundation rests on soft soil [7-9]. The effects of soil-structure interaction (SSI) on piled foundations include [10]: (i) kinematic bending applied along the piles - even in the absence of a superstructure, (ii) the variation between the free-field ground motion and the motion at the pile top, i.e. at the base of the superstructure. Numerous and detailed technical reviews have been published on such SSI effects [11-16]. As kinematic and inertial interactions are not synchronous, an adequate combination rule of the corresponding effects should be defined, but this is beyond the scope of this paper. Modern codes of practice worldwide [17-20] include pile design provisions that account for the effects of both mechanisms; they provide simplified expressions for

evaluating the period elongation due to the soil-structure interaction. Such rules, which are primarily theoretically-based, refer to a limited number of foundation layouts and soil types, thus requiring further investigations and generalization. Laboratory investigations are essential for studying the complex soil-structure interaction, as actual field data are scarce and full scale tests are expensive to conduct and often difficult to interpret [21]. While data from instrumented piles under buildings of different vibrational characteristics subjected to actual earthquake motions would be ideal, such data are rare due to high cost and the unpredictable nature of earthquake occurrence. Therefore, well-controlled laboratory investigations on pile models alongside with analytical and numerical simulations are pivotal for understanding the seismic response of both single piles and pile groups [22-29].

The scope of the present work is to examine the complex soil-pile-structure interaction problem by discussing in a detailed manner a large set of experimental results of high-quality shaking table tests carried out on pile models. The experimental program was performed at the Bristol Laboratory for Advanced Dynamics Engineering (BLADE), within the Framework of the Seismic Engineering Research Infrastructures for European Synergies (SERIES), which was funded by the 7th Programme of the European Commission.

Experimental tests were carried out on different pile group configurations, with and without pile caps and/or superstructures, subjected to both horizontal and vertical dynamic shaking. The loading conditions presented in this paper include white noise and harmonic excitations. The tests aimed at investigating experimentally the fundamental and critical issues of seismic Soil-Pile-Structure-Interaction (SPSI). Primary focus is on the dynamic response of the systems, namely natural frequencies and damping ratios, as a function of the pile configurations and the amplitude of white noise excitations. Such response parameters are of primary interests for structural engineers as they may affect significantly the evaluation of the demand on structural systems, especially in earthquake prone regions and under high winds. Moreover, the influence of the oscillator masses for both pile configurations on pile response has been analysed; in so doing sinusoidal input motions have been considered in the shake table tests.

2. Experimental setting

The dynamic response of a single pile and a pile group was explored by means of 1-g shaking table tests, using the 6-degree-of-freedom earthquake simulator of BLADE. To this end, a shear stack was employed to simulate the soil behaviour, as further discussed hereafter.

Shaking table testing facility

The 6-degree-of-freedom shaking table at BLADE, which has been used within the EU-funded SERIES testing program, consists of a 3m x 3m cast-aluminium seismic platform capable of carrying a maximum payload of 21 t. The platform is mounted within a 100 t concrete block secured to bedrock. It is driven horizontally and vertically by eight 70 kN servo-hydraulic actuators of 0.3m stroke length giving full control of motion of the platform. The table is powered by five pairs of hydraulic pumps capable of delivering 900 l/min at a working pressure of 230 bar. The operative frequency range is $0 - 100$ Hz.

The soil used for the experimental tests was contained in the laminar equivalent shear beam container (ESB), as shown in Figure 2. The ESB consists of 8 rectangular aluminium rings, which are stacked alternately with rubber sections to create a hollow flexible box of inner dimensions 1.190 m long by 0.550 m wide and 0.814 m deep [30]. The rings are made of aluminium box section to minimize inertia while providing sufficient constraint for the K_0 condition. The stack is secured to the shaking table by its base and shaken horizontally lengthways (y direction). Its floor is roughened by sand-grain adhesion to improve the shear wave transfer; the internal end walls are similarly treated to enable complementary shear stresses. Internal side of walls are lubricated with silicon grease and covered with latex membrane to ensure plane strain conditions. The resonant frequency and damping ratio of the empty container in the first shear mode in the long direction

were measured prior to testing as 5.7 Hz and 27%, respectively. The latter values are sufficiently different from the values obtained for the container filled of soil material [28-30].
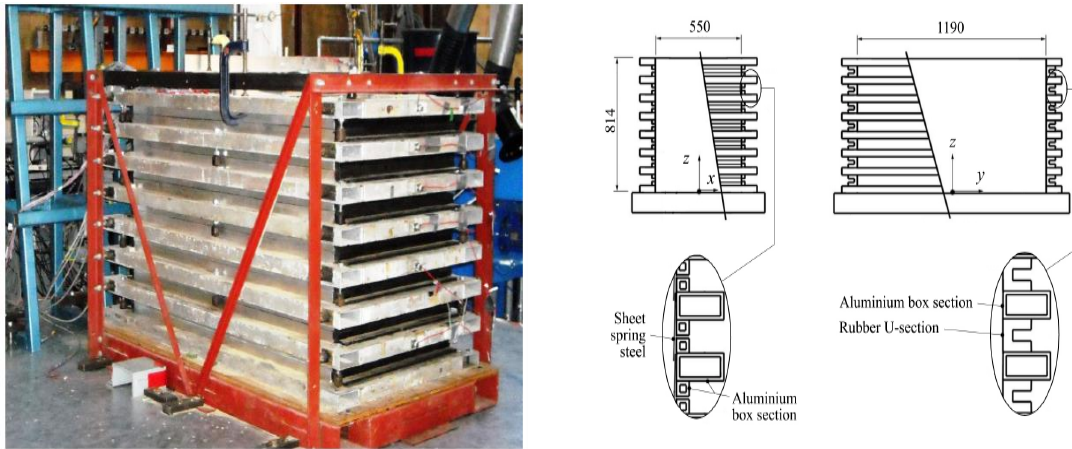

Figure 2. Equivalent shear beam container (shear stack) of BLADE

Scaling laws for prototype and model configuration

The prototype pile used for the SERIES testing program is a concrete pile of Young's modulus E_p=25 GPa, diameter d=600 mm and length L=20 m. The pile is embedded in a two-layer soil deposit. Each soil layer is characterized by its thickness h, density ρ, shear wave velocity V_s, Poisson's ratio ν, and damping ratio D. The prototype shear wave velocities are V_{s1}=100 m/s and V_{s2}=400 m/s for the upper and the lower layer, respectively.

The typical problem with the small scale modelling lies in its limited ability to satisfy the laws of physical and geometrical similarity between the model and the prototype. However, its effectiveness depends on whether all the relevant factors that influence the behaviour of the prototype have been captured in the model. Muir Wood et al. [23] derived a number of scaling factors for single and n-g gravity soil models from four fundamental scaling factors (length, density, stiffness and acceleration). From the scale factor for length, all remaining model parameters can be derived (Table 1). In this study, the ratio between the prototype soil thickness (30 m) and the height of the test container (0.8 m) provides the fundamental scale factor for length (n=37.5) The soil shear wave velocities at model scale would be $V_{s1} = 40$ m/s and $V_{s2} = 160$ m/s, which may lead to a model stiffness ratio G_{bottom}/G_{top} of 16. However the shear wave velocity obtained by the experimental soil deposition procedure were somewhat different than the target values, giving a different stiffness ratio.

Table 1. Scale factors for the sample model (after [23])

Variable	Scale Factor	Magnitude
Length	$Length_{model}/ Length_{prototype} = n_l$	$1/n$
Density	n_ρ	1
Stiffness	n_G	$1/\sqrt{n}$
Acceleration	n_g	1
Stress	$n_\rho\, n_g\, n_l$	$1/n$
Strain	$n_\rho\, n_g\, n_l\, /n_G$	$1/\sqrt{n}$

Displacement	$n_\rho\, n_g\, n_l^2\, /n_G$	$1/n^{1.5}$
Velocity	$n_g\, n_l\, \sqrt{(\,n_\rho/n_G)}$	$1/n^{0.75}$
Dynamic time	$n_l\, \sqrt{(\,n_\rho/n_G)}$	$1/n^{0.75}$
Frequency	$\sqrt{(\,n_G\,/n_\rho)}/\,n_l$	$n^{0.75}$
Shear wave velocity	$\sqrt{(\,n_G\,/n_\rho)}$	$1/n^{0.25}$

Sample model

The SERIES test campaign consisted of two series of tests: preliminary tests (Phase I) and a subsequent more comprehensive set, also including earthquake loading (Phase II).

The sample model consists of five piles embedded in a bi-layer soil (Figure 3). Each pile is an alloy aluminium tube (commercial model 6063-T6) with thickness t = 0.71 mm, outer diameter D = 22.23 mm and length L = 750 mm. The main properties of the aluminium tube are reported in Table 2.

Pile 3, 4 and 5 are closer to each other with a relative spacing s=70 mm (s/D ≈ 3); pile 1 and 2 are placed at higher distance, equal to 140 mm. The superstructure is a single degree of freedom (SDOF) system. It consists of two different types of columns (aluminium and steel) with extra masses added to its top to achieve different dynamic response. The fundamental properties of the sample SDOF column are listed in Table 2. Details of the fixed base oscillator properties are shown in Table 3.
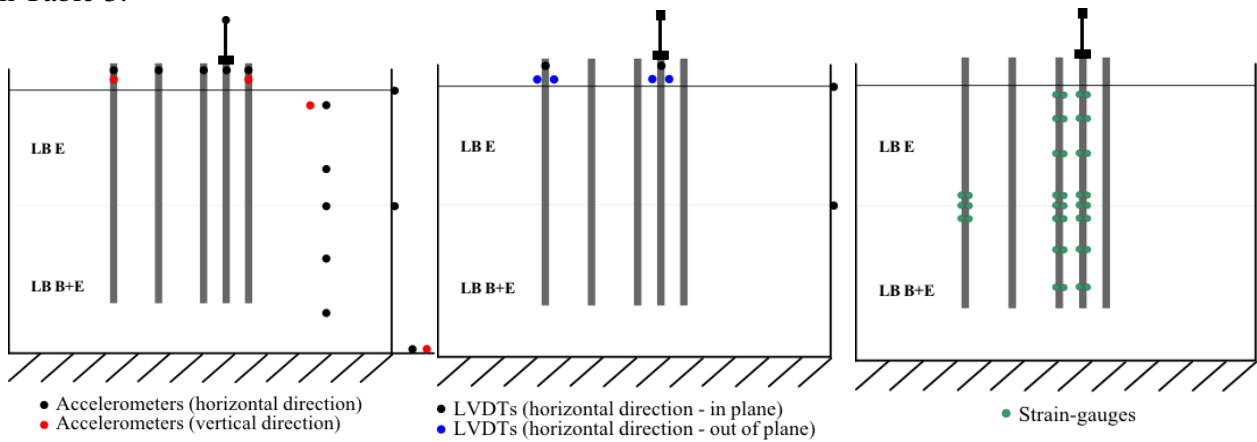

- Accelerometers (horizontal direction)
- Accelerometers (vertical direction)
- LVDTs (horizontal direction - in plane)
- LVDTs (horizontal direction - out of plane)
- Strain-gauges

Figure 3. Model setup: accelerometers, LVDTs and strain gauges locations

Table 2. Pile and column characteristics

Element [type]	Geometrical details [mm]	*Unit weight* [kN/m^3]	*Length* [mm]	Young's modulus E [GPa]
Pile	D_e = 22.23 t = 0.71	27	750	70
Aluminum column (rectangular section)	Cross section 3x12	27	100 (Phase I) 50 -100 (Phase II)	70
Steel column (rectangular section)	Cross section 3x12	80	100 (Phase II)	21

4

Instrumentation

Accelerometers, totalling 18, were used to monitor the accelerations of the shaking table, the shear stack, the soil along a vertical array, the pile heads and the superstructure. Eight Linear Variable Displacement Transformers (LVDTs) were employed to monitor the displacements of the pile in the horizontal and vertical directions. Bending response along piles has been evaluated by strain gauges attached on pile shafts: eight pairs of instruments have been placed along piles 4 and 5, while only 4 strain gauges have been attached on pile 1, close to the layer interface. The location of all the instruments is reported in Figure 3. Overall, 63 data channels were employed.

Soil material properties

A two-layer soil deposit was obtained by pluviation. The top layer was made of Leighton Buzzard sand (LB) fraction E, the bottom layer is a mix between LB fractions B and E (85% and 15%, respectively). The free surface of the soil deposit is 800mm above the base of the shear stack. The LB sand adopted herein has been extensively used in the experimental research activity carried out at the BLADE. Numerous density and stiffness data can be found in experimental studies existing in the literature on similar soils [31-35]. Table 4 outlines the sand index properties used in some of the cited studies.

Table 3. Properties of the sample oscillators

Column details	Total added mass [g]	Fixed base frequency (f) [Hz]	Damping ratio [%]
Aluminium h=100mm (Phase I)	75	38.00	0.70
	125	30.50	1.20
	175	26.50	0.90
	275	20.50	1.40
	475	15.00	1.20
	975	10.40	1.50
Aluminium h=100mm (Phase II)	75	36.28	0.75
Aluminium h=50mm (Phase II)	150	27.02	0.59
Steel h=100mm (Phase II)	300	20.37	0.45

Table 4. LB sand index properties

Materials	Type	G_s [Mg/m^3]	e_{min}	e_{max}	D_{10}	D_{50}	References
LB - fraction E	Sand BS 881-131	2.647	0.613	1.014	0.095	0.140	Tan (1990)

LB - fraction B	Sand BS 881-132	2.647	0.486	0.780	0.820	Ling and Dietz (2004)
LB - fraction E+B		2.647	0.289	0.614		Moccia (2009)

The shear wave velocity Vs values were derived from the white noise tests carried out before the sinedwell and earthquake tests for each stage of the experimental programme. Starting from the experimentally measured natural frequencies of the whole deposit and the top layer, and using the closed form solution proposed in [36], the shear modulus variation with depth in the bi-layer deposit is evaluated (assuming the typical average value of 0.5 for the corresponding power-law dependence for sand) and used for the evaluation of the shear wave velocity profile. The initial shear wave velocity contrasts between the bottom (Vs2) and top layer (Vs1) obtained in the two experimental phases are quite close, around 1.6, for the two stages of tests (Table 5).

Table 5. Soil layer properties

Soil layers	Thickness H (mm)	Dry unit weight γ_d (kN/m3)		Shear wave velocity [36] V^*_s (m/s)		V^*_{s2}/V^*_{s1}	
		Phase I	Phase II	Phase I	Phase II	Phase I	Phase II
Top LB(E)	340	13.63	13.13	51	54	1.59	1.57
Bottom LB(E+B)	460	17.46	17.92	81	85		

Pile configurations

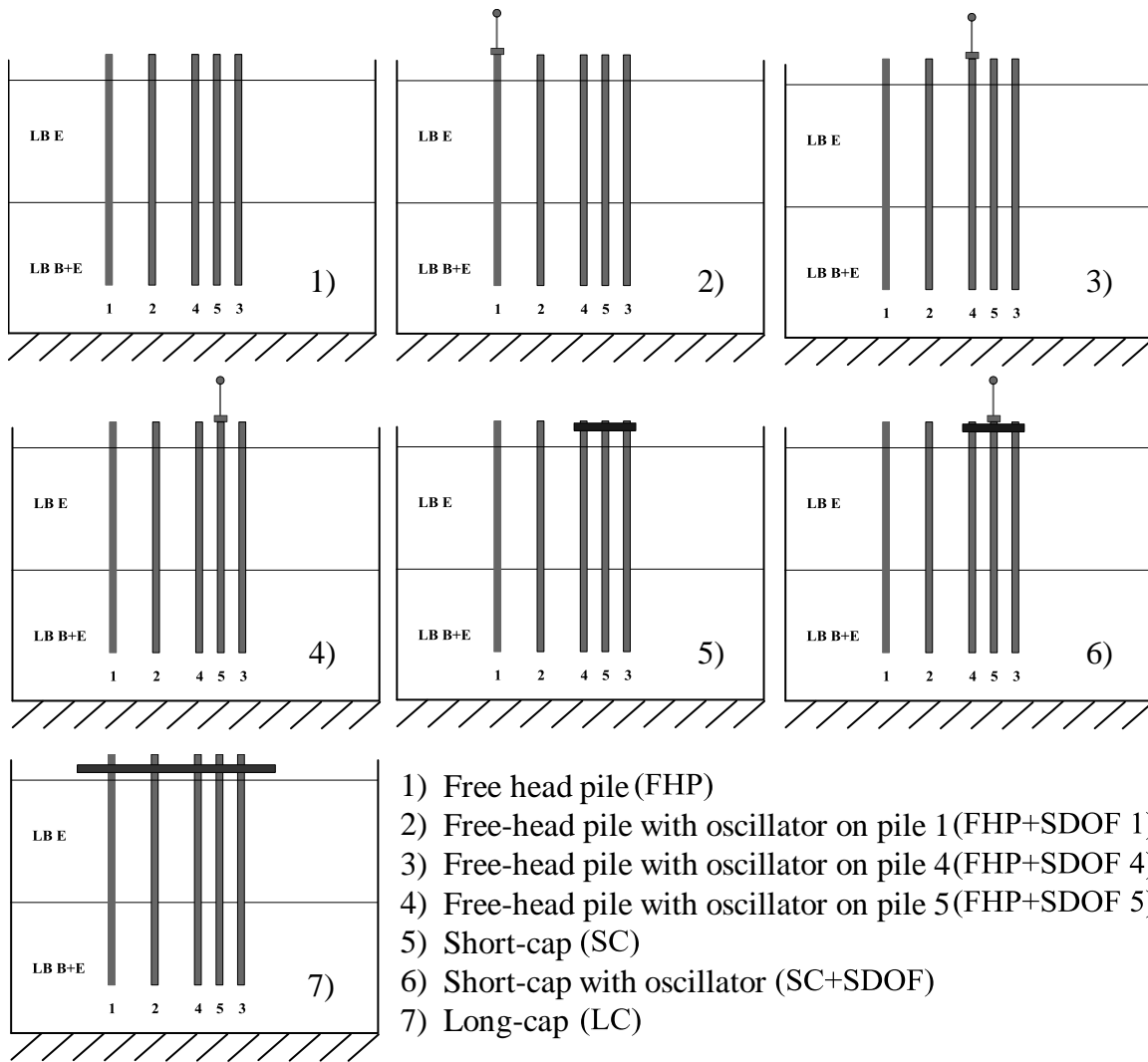Seven different model configurations, as displayed in Figure 4, were tested starting from the model setup of Figure 3.

6

Figure 4. Details of model configurations

1) Free head pile (FHP)
2) Free-head pile with oscillator on pile 1 (FHP+SDOF 1)
3) Free-head pile with oscillator on pile 4 (FHP+SDOF 4)
4) Free-head pile with oscillator on pile 5 (FHP+SDOF 5)
5) Short-cap (SC)
6) Short-cap with oscillator (SC+SDOF)
7) Long-cap (LC)

Details of the set-up of two configurations of the physical models assembled at BLADE are shown in Figures 5 and 6. Figure 5 depicts configuration 4, characterized by free-head piles and one oscillator placed on Pile 5 (Free Head Pile plus Single Degree Of Freedom - FHP+SDOF). Figure 6 shows configuration 6, characterized by a small cap connecting piles 4, 5 and 3, with an oscillator mounted on the top of the central pile (pile 5) (Short Cap plus Single Degree Of Freedom - SC+SDOF).
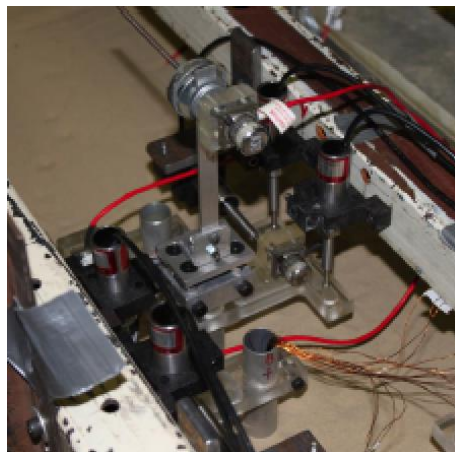

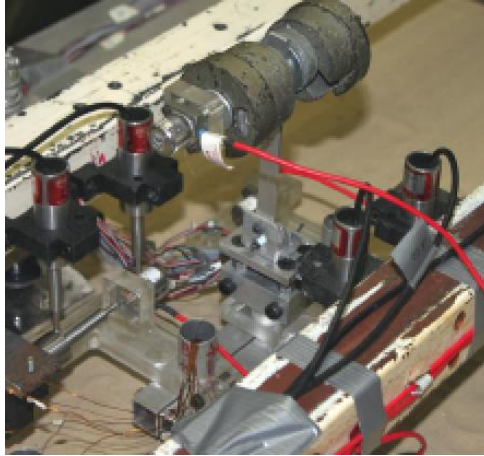*Figure 5. Oscillator on Free Head Pile configuration (FHP+SDOF)*

Figure 6. Close up of the Oscillator on Short Cap configuration (SC+SDOF)

Experimental test protocol and input motion

More than 600 shaking tests were carried out during the experimental campaign: 366 tests in Phase I and 248 tests in Phase II. Horizontal white noise and sinedwell inputs were utilised for the first set of preliminary tests, whereas a comprehensive set of input motions, including vertical white noise, sinedwells, earthquake records, snapback and pullover tests were adopted for the second phase. The experimental loading testing protocol included the following input motions:

- *White noise input*: during white noise exploratory testing, random noise signals of bandwidth 0-100 Hz and peak ground acceleration varying between 0.01 g and 0.10 g were employed.
- *Harmonic input*: sinedwell acceleration time-histories were imposed. In the first stage each sinedwell involved 12 steady-state cycles; 15 different frequencies of excitation (varying from 5 to 30 Hz with a step of 2.5 Hz, and from 30 to 50 Hz with a step of 5 Hz) and acceleration amplitudes varying between 0.01-0.18g were applied. In the second stage of the experiments, the sinusoidal excitation encompassed 16 steady cycles; 7 frequencies (varying from 5 to 45 Hz with a step of 5 Hz) were employed, with acceleration amplitudes varying between 0.01-0.13g.

3. Test results

The outcomes of typical tests of the experimental program are discussed hereafter. The primary aim is to investigate the soil-structure-interaction effects on: *(i)* the natural period of vibration of the sample SDOF oscillator under white noise excitations, and *(ii)* pile response under harmonic input motions.

3.1. Soil-structure interaction effects

In order to investigate the effects of soil-structure interaction on the natural vibration period of the oscillators, several tests were carried out on different system configurations. Such tests were aimed at assessing the effects on the global system response of both the input motion (type of excitation and amplitude) and SDOF oscillator masses.

Preliminary white noise tests were conducted in order to determine experimentally the "fixed base" frequency (f) and damping ratio (D) of the oscillator, by connecting it rigidly to the shaking table floor (Table 3). The observed increase of damping ratio with mass could be attributed to the relative movement between the elements added at the top of the column to form the desired mass.

Modal analysis response of the six fixed-base oscillators (tested in Phase I) have been assessed by using the finite element computer program SAP2000 [37]. Table 6 shows that the natural frequencies obtained from the numerical analyses are slightly higher than the experimental counterparts. The approximation is however acceptable for the scope of the present work: the computed variations range between 7% and 14%.

8

Table 6. Experimental test and numerical simulation results: frequency and damping of fixed-base oscillators

Total added mass [g]	Mass elements	Fixed base frequency (f) [Hz]		Discrepancy (M) − (C) [%]	Damping ratio [%]
		Measured (M)	Computed (C)		
75	Mass-fixing device and accelerometer	38.0	43.7	+13.0	0.7
125	Mass-fixing device and accelerometer + 50g	30.5	33.9	+10.0	1.2
175	Mass-fixing device and accelerometer + 2 x 50g	26.5	28.6	+7.3	0.9
275	Mass-fixing device and accelerometer + 4 x 50g	20.5	22.8	+10.1	1.4
475	Mass-fixing device and accelerometer + 8 x 50g	15.0	17.4	+13.8	1.2
975	Mass-fixing device and accelerometer + 2 x 50g + 4 x·200g	10.4	12.1	+14.0	1.5

The soil-pile-structure interaction effects are analysed with reference to the two different pile-head configurations, namely free-head pile (FHP+SDOF) and short-cap (SC+SDOF), as depicted in Figure 7.
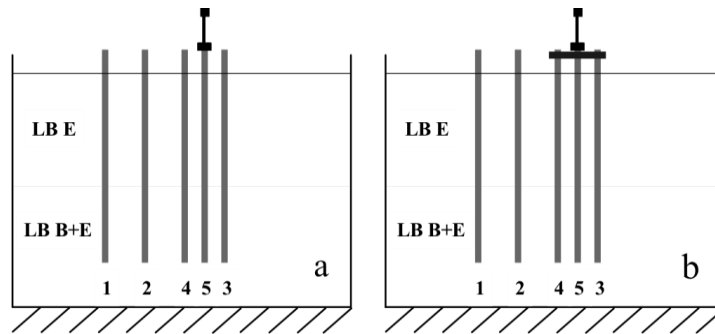

Figure 7. Model configurations considered: (a) FHP+SDOF, (b) SC+SDOF

The aim is the evaluation of the period shifting and the damping ratio of the whole system (soil, pile and superstructure) with respect to the experimental fixed base oscillator.

The Transfer Functions (TFs) between signals recorded on different components of the whole experimental model have been computed for evaluating the following dynamic responses:

- *the system response referred to the shaking table*, computed as the ratio between the FFT of the accelerogram at the top of the oscillator and the FFT of the one at the shaking table;
- *the oscillator response*, computed by the ratio between the Fast Fourier Transform (FFT) of the accelerogram at the top of the oscillator and that at the bottom of the oscillator (corresponding to the top of pile 5)*;*
- *the system response referred to the free-field condition*, computed as the ratio between the FFT of the accelerogram at the top of the oscillator and the FFT of the one at the soil surface.

The above mentioned TFs allow estimating the fundamental frequencies of the whole system (f_{SSI}) and those relative to its parts. The response of the oscillator placed on pile 5 in the FHP+SDOF configuration (Figure 7a) is examined hereafter. The amplitude of the adopted excitations varied between 0.02g and 0.08g. Figure 8 shows the estimated transfer functions between the oscillator and the SDOF base (Figure 8a), and the oscillator and the free-field (Figure 8b) for the white noise

motion with maximum acceleration equal to 0.02g. The amplification values are significantly higher for the ratio between the SDOF and its base respect to the one referred to the free-field. This outcome confirms that the acceleration time history at foundation level (pile top) shows lower amplitudes, as expected.
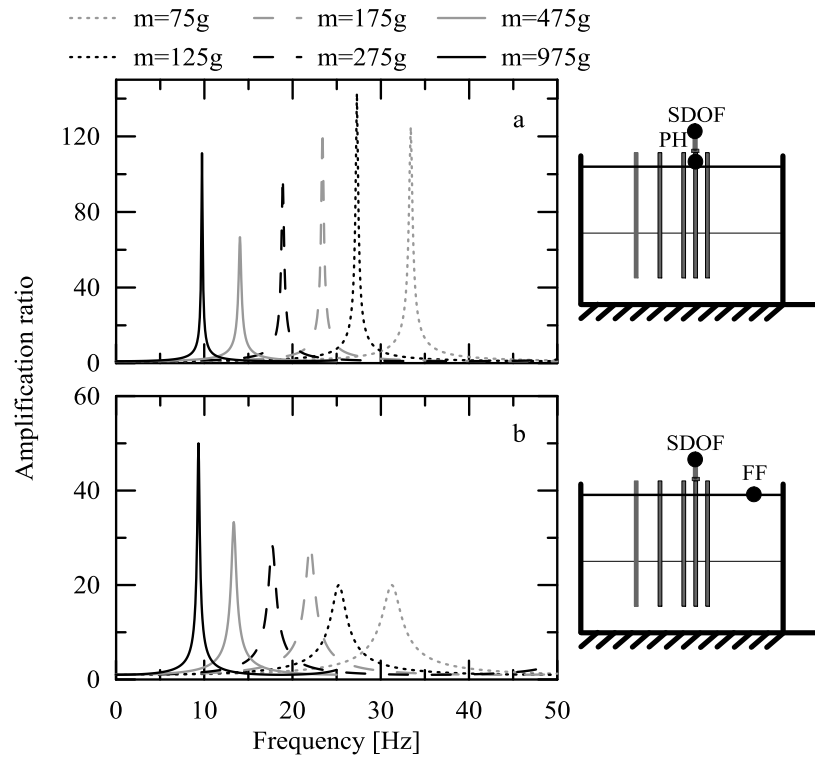

Figure 8. FHP+SDOF configurations: transfer functions referred to (a) SDOF base and (b) free-field for all the oscillator masses (white noise test: $a_{max}=0.02g$*)*

In order to investigate the effects of seismic soil-pile-structure interaction (SSPSI) on SDOF response referred to shaking table (ST), free field (FF) and pile head (PH), the shifting of the SDOF fundamental frequencies (and periods) with respect to the SDOF fixed-base configuration has been evaluated. The values for the two white noise inputs with maximum accelerations 0.02g and 0.08g, and for the different tested masses are summarized in Table 7. The results show that, due to the soil-pile-structure interaction, the natural frequencies are not close to the "fixed base" counterparts.

Similar analyses have been carried out for the short-cap configuration (SC+SDOF, Figure 7b). The amplitude of white noise excitations varied between 0.02g and 0.08g. Figure 9 displays the plots of such TFs for the input motion with maximum acceleration equal to 0.02g, computed with reference to the SDOF base (Figure 9a) and the free-field (Figure 9b). The natural frequencies are close to the fixed-base ones. This is anticipated due to the high stiffness of the cap device.

Table 7. FHP+SDOF configurations: period shifting for the sample systems

mass [grams]	Transfer function	a ~ 0.02g				a ~ 0.08g			
		f [Hz]	T_{SSI} [s]	ΔT [%]	D_{SSI} [%]	f [Hz]	T_{SSI} [s]	ΔT [%]	D_{SSI} [%]
75	SDOF-ST	31.00	0.032	22.58	2.90	30.60	0.033	24.18	1.60

	SDOF-FF	31.25	0.032	21.60	5.00	30.60	0.033	24.18	3.50
	SDOF-PH	33.40	0.030	13.77	0.80	33.65	0.030	12.93	0.50
	SDOF-ST	25.40	0.039	20.08	2.75	24.60	0.041	23.98	2.64
125	SDOF-FF	25.25	0.040	20.79	5.00	24.75	0.040	23.23	3.50
	SDOF-PH	27.30	0.037	11.72	0.70	27.10	0.037	12.55	0.50
	SDOF-ST	22.00	0.045	20.45	3.18	21.50	0.047	23.26	1.86
175	SDOF-FF	22.00	0.045	20.45	3.50	21.50	0.047	23.26	2.50
	SDOF-PH	23.40	0.043	13.25	0.80	23.33	0.043	13.59	0.50
	SDOF-ST	17.70	0.056	15.82	1.13	17.35	0.058	18.16	1.73
275	SDOF-FF	17.70	0.056	15.82	3.50	17.40	0.057	17.82	3.00
	SDOF-PH	18.90	0.053	8.47	1.00	18.65	0.054	9.92	1.00
	SDOF-ST	13.30	0.075	12.78	2.00	13.18	0.076	13.81	1.50
475	SDOF-FF	13.35	0.075	12.36	3.00	13.10	0.076	14.50	3.00
	SDOF-PH	14.05	0.071	6.76	1.50	13.90	0.072	7.91	1.50
	SDOF-ST	9.40	0.106	10.64	1.50	9.15	0.109	13.66	1.50
975	SDOF-FF	9.35	0.107	11.23	2.00	9.10	0.110	14.29	3.00
	SDOF-PH	9.75	0.103	6.67	0.90	9.60	0.104	8.33	2.00

Keys: ST shaking table; FF free-field; PH Pile head; $\Delta T = (T_{SSI} - T)/T$
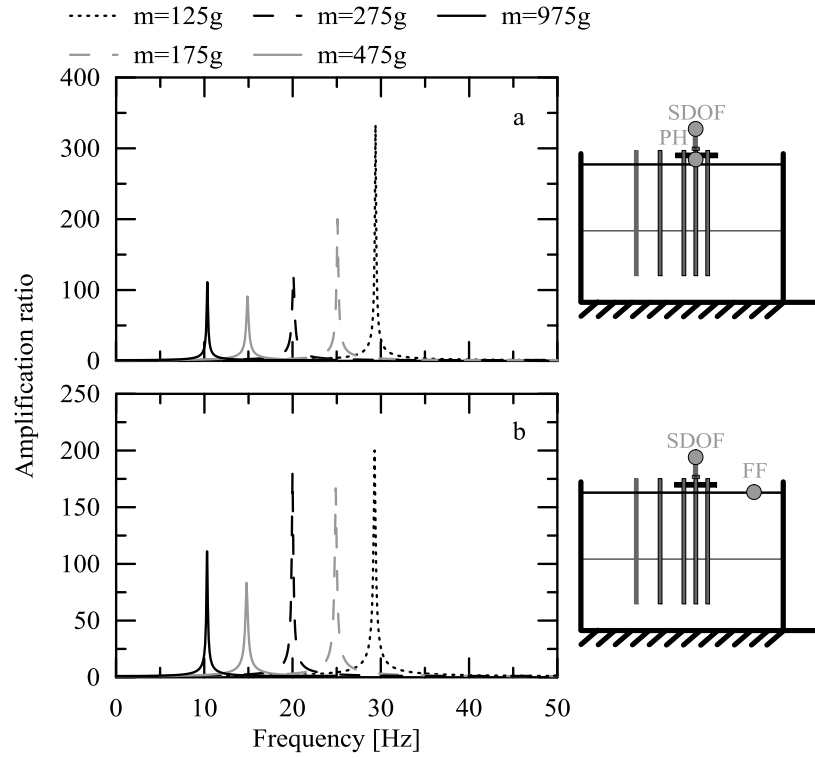
Figure 9. SC+SDOF configurations: transfer functions referred to (a) SDOF base and (b) free-field for all the oscillator masses (white noise test: $a_{max}=0.02g$*)*

The computed results for three white noise excitations with maximum accelerations 0.02g, 0.04g and 0.08g and for the different tested masses are summarized in Table 8, with reference to shaking table (ST), free field (FF) and pile head (PH).

Table 8. Period shifting for the sample systems in the SC+SDOF configurations

mass [grams]	Transfer function	White noise a ~ 0.02g				White noise a ~ 0.04g				White noise a = (0.07÷0.09)g			
		f [Hz]	T_{SSI} [s]	ΔT [%]	D_{SSI} [%]	f [Hz]	T_{SSI} [s]	ΔT [%]	D_{SSI} [%]	f [Hz]	T_{SSI} [s]	ΔT [%]	D_{SSI} [%]
	SDOF-ST	29.30	0.034	4.10	0.08	29.15	0.034	4.63	0.30	29.15	0.034	4.63	0.20
125	SDOF-FF	29.30	0.034	4.10	0.50	29.18	0.034	4.52	0.50	29.15	0.034	4.63	0.50
	SDOF-PH	29.40	0.034	3.74	0.30	29.35	0.034	3.92	0.50	29.35	0.034	3.92	0.50
	SDOF-ST	24.90	0.040	6.43	0.16	24.85	0.040	6.64	0.15	24.80	0.040	6.85	0.20
175	SDOF-FF	24.90	0.040	6.43	0.60	24.90	0.040	6.43	0.50	24.85	0.040	6.64	0.50
	SDOF-PH	25.10	0.040	5.58	0.50	25.00	0.040	6.00	0.50	25.00	0.040	6.00	0.50
	SDOF-ST	20.00	0.050	2.50	0.30	19.90	0.050	3.02	0.17	19.85	0.050	3.27	0.20
275	SDOF-FF	20.00	0.050	2.50	0.55	19.95	0.050	2.76	0.50	19.90	0.050	3.02	0.80
	SDOF-PH	20.10	0.050	1.99	0.80	20.05	0.050	2.24	0.50	20.00	0.050	2.50	1.00
	SDOF-ST	14.80	0.068	1.35	1.10	14.70	0.068	2.04	0.80	14.70	0.068	2.04	0.50
475	SDOF-FF	14.80	0.068	1.35	1.20	14.70	0.068	2.04	1.50	14.75	0.068	1.69	1.50

	SDOF-PH	14.90	0.067	0.67	1.10	14.80	0.068	1.35	1.50	14.80	0.068	1.35	1.50
	SDOF-ST	10.30	0.097	0.97	1.50	10.25	0.098	1.46	1.50	10.15	0.099	2.46	1.50
975	SDOF-FF	10.32	0.097	0.78	0.90	10.28	0.097	1.17	0.80	10.20	0.098	1.96	1.00
	SDOF-PH	10.35	0.097	0.48	0.90	10.30	0.097	0.97	0.90	10.20	0.098	1.96	1.00

Keys: ST shaking table; FF free-field; PH Pile head; $\Delta T=(T_{SSI}-T)/T$

The results of the period elongation (T_{SSI}/T) and damping ratio (D_{SSI}/D) for the sample input motions in the two configurations (referred to free-field) are summarised in Figure 10. The results are plotted versus the so-called wave parameter $(1/\sigma)$ (Eq. 1), an index of the structure and soil relative stiffness [38-20]. The V_s considered in the equation is, as a first approximation, the one in a depth equal to the active length of the pile - which lies in the top layer for the cases in hand. The wave parameter is expressed as follows:

$$ \tag{1} $$

According to theory [10, 39, 40] the aforementioned dimensionless parameter influences significantly the SSI effects in seismic structural response. The increase of the SSI effect with the wave parameter for both configurations is evident. Figure 10a, shows the data and the corresponding fitting curve for each configuration and indicates an approximately linear variation of the period elongation with $(1/\sigma)\cdot$. Due to group action of the piles in the SC+SDOF configuration, the period elongation is significantly lower than for the FHP+SDOF configuration. Evidently, the connection tends to replicate the fixed base condition for the oscillator. It is also worth noting that the linear regressions in the graph match only approximately the condition of no frequency shift at $(1/\sigma) = 0$. Several analytical solutions have been proposed to estimate the period elongation due to SSI for both piles [41-42] and footings [43-45]. The comparison of analytical results with the experimental counterparts lies beyond the scope of the present paper and will be explored in a future publication.

In order to evaluate the variation of the damping ratio for the two sample configurations, it is necessary to consider the occurrence of soil material damping and radiation damping. The latter phenomenon is related to the different stiffness between pile and surrounding soil as well as the difference in volumes: piles tend to vibrate at higher frequencies and emit high frequency energy away into the soil in the form of stress waves, which travel far from source (to infinity in an unbounded medium). This effect is amplified by the presence of pile cap that makes the structural system stiffer. Figure 10b shows the variation in terms of damping ratio for the FHP+SDOF configuration, referring to the total system damping divided by the fixed-base experimental value.

The increase in damping ratio with $(1/\sigma)$ is evident in the graph. The general trend of damping ratio, that increases with the wave parameter and depends on the input acceleration, seems to be not affected by the radiation damping. Conversely, such phenomenon becomes dominant in the SC+SDOF configuration and makes not clear the variation of the measured damping ratio.
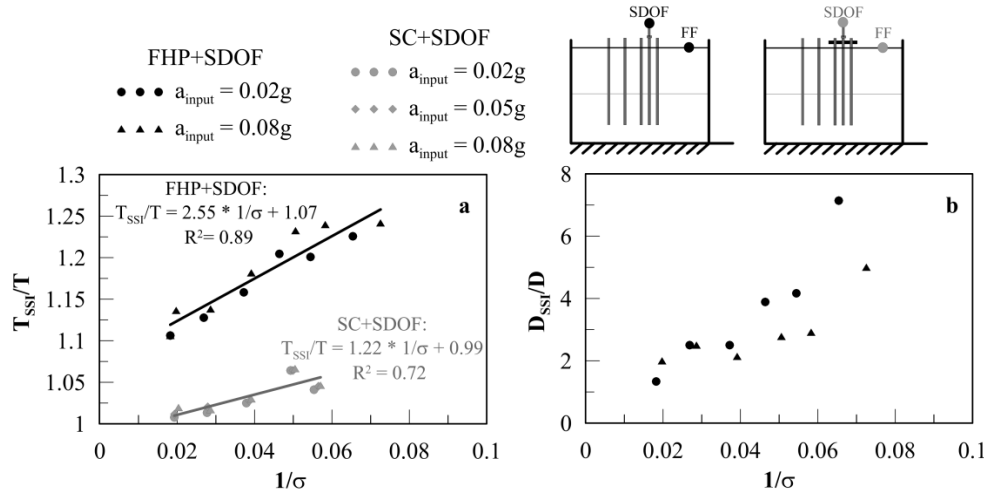
Figure 10. Dynamic response of the system: (a) period elongation and (b) damping ratio versus wave parameters for FHP+SDOF (in black) and SC+SDOF (in grey) configurations

Referring to the oscillator mass giving the maximum period elongation in the SC+SDOF configuration (m=175g), Figure 11 shows the transfer functions computed with reference to the SDOF base (Figure 11a) and the free-field (Figure 11b) for white noise of 0.02g amplitude. The SC+SDOF configuration gives a very low elongation (around 6%), while in the FHP+SDOF configuration it reaches a value of 20%, considering the complete SSPI (referred to the free-field signal).
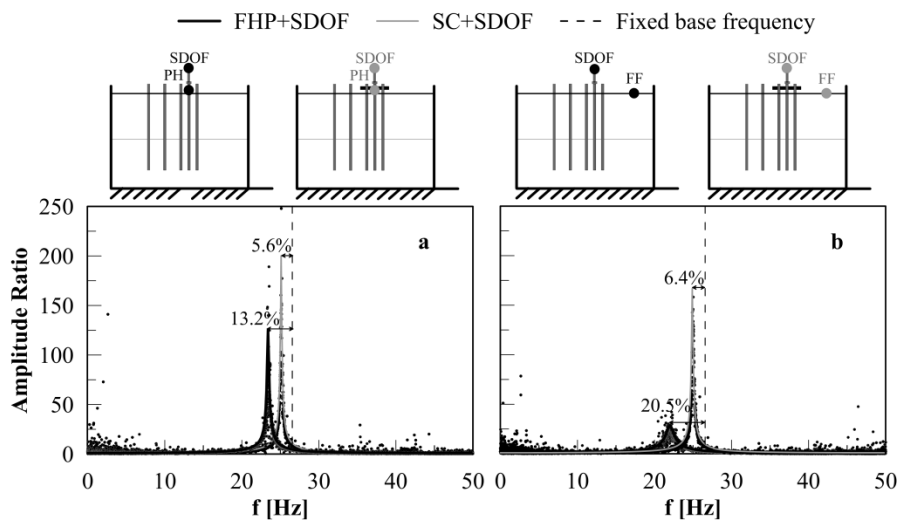
Figure 11. FHP+SDOF and SC+SDOF configurations: comparison of transfer functions with respect to (a) the SDOF base and (b) free-field (white noise test: $a_{max}=0.02g$; m= 175g)

3.2. Pile response

The effects of period elongation on the response of the pile in the FHP+SDOF (Figure 7a) and SC+SDOF configurations (Figure 7b) are presented in this section with reference to harmonic input motions. The results illustrated hereafter refer to an input frequency of 20 Hz and amplitude at the shaking table equal to 0.1g.

3.2.1. Free-head pile + single degree of freedom configuration

The response of the soil obtained in several tests with different SDOF mass configurations is illustrated in Figure 12a, where maximum accelerations of a soil column far enough from piles, so as to be considered unaffected from them (in the so called free-field condition), are plotted as a function of depth. In such tests, the soil response does not vary, hence it should produce the same kinematic interaction effects on the piles. As a consequence, the variations observed in the response

14

of piles should be related only to the inertial effects induced by the SDOF masses.

Starting from the response of the strain-gauges located along the instrumented piles (pile 4 and 5), the bending moment time-histories have been computed [46], assuming the conservation of the plane section and elasticity of pile. Piles response are evaluated in terms of "strain transmissibility" of the system computed as the ratio between the pile bending strain (ε_p), defined in [1], and the characteristic shear strain (γ_c), defined in [2]:

$$\varepsilon_p = \frac{Md}{2E_p I_p} \tag{2}$$

$$\gamma_c = \frac{\rho_1 h_1 a_s}{G_1} \tag{3}$$

where a_s is the peak ground acceleration at the surface.

As far as pile 5 is concerned, the inertial effects induced by the SDOF are maximum at the pile head and significant up to a depth that is a function of the mass value. It is worthwhile to consider the dynamic response of the system: the increase of the maximum strain transmissibility at the pile head (ε_{PH}) is related to the resonance condition. The above outcome is illustrated in Figure 13, in which (ε_{PH}) for pile 5 is plotted versus the ratio between the input fundamental frequency and the frequency of the system. As regards the system frequency, two different values have been determined: the first one, quoted as structural frequency (f_s), which refers to the frequency of the oscillator, is obtained from the transfer function between the top of the oscillator and its base (the head of the pile); the second frequency takes into account SSI and is obtained from the transfer function between the top of the oscillator and the free-field (f_{SSI}). Figure 13 shows the maximum strain transmissibility at the pile head referring to structural frequency (Figure 13a) and free-field response (Figure 13b). For SDOF mass of 175g the frequencies are f_s = 22.2 Hz and f_{SSI} = 18.6 Hz; considering the input motion frequency (20 Hz), it is possible to verify the onset of the resonance for all sample masses. Hence the maximum strain transmissibility at the pile head is not an increasing function of the SDOF mass: as a matter of fact, the minimum value is observed for the highest mass (m=975g), which is farthest from resonance ($f_{input}/f_{SSI} \approx 2$).

The envelopes of absolute strain transmissibility with respect to γ_c along piles 4 are plotted in Figure 12b. The experimental results show that also for pile 4 the maximum bending values are achieved for the resonance condition between the closely-located pile 5 (and SDOF) system and the input motion. The maximum values again occurs in the test with the oscillator mass equal to 175g. The maximum strain trasmissibility values, achieved for all the tests at the same depth, vary significantly with the mass of the oscillator (even by a factor of 100%): this effect is related to the difference in phase between pile 4 and pile 5 displacements. It is important to notice that the location of the maximum bending values is clearly located at a lower depth in all the sample case studies (Figure 12b).
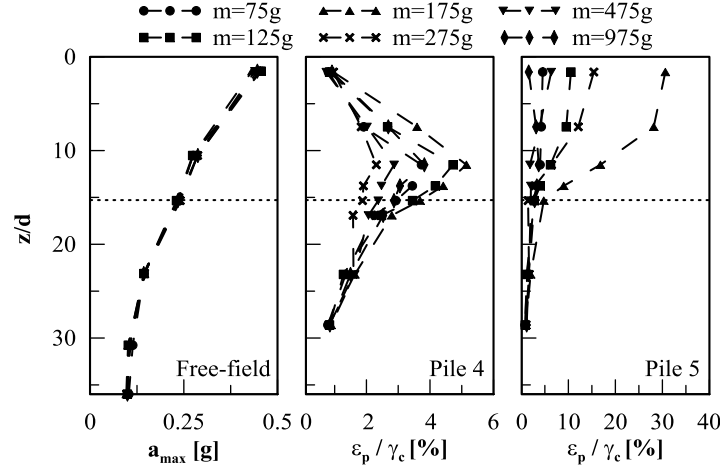
Figure 12. FHP+SDOF configuration: envelope of free-field accelerations and bending moments along piles 4 and 5 (sinedwell test: f=20 Hz, a_{max}=0.1g)
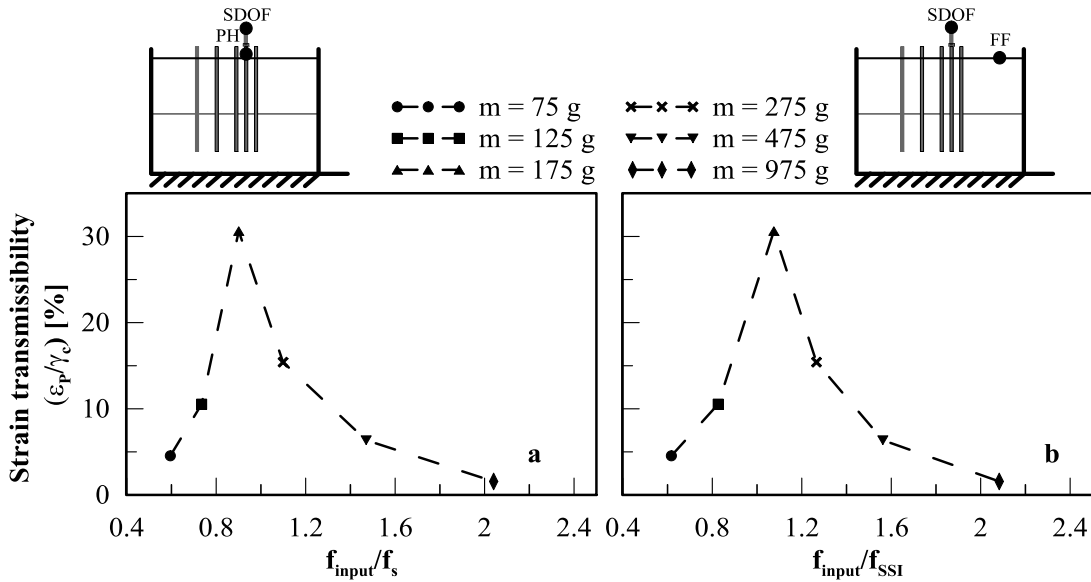

Figure 13. FHP+SDOF configuration: maximum strain transmissibility at pile 5 head versus the ratio between (a) the input and the pile head and (b) the input and the SSI frequency for pile 5 (sinedwell test: f=20 Hz, a_{max}=0.1g)

The influence of resonance on the response of pile 4 is illustrated in Figure 14. The strain transmissibility curves along pile 4 are compared for the two configurations considered in this paragraph: FHP without the oscillator (20 Hz input motion frequency, a_{max}= 0.09g) and FHP+SDOF on pile 5 (20 Hz input motion frequency, a_{max}= 0.10g). In the FHP configuration the location of the maximum bending moment is, as expected, very close to the layer interface. In the FHP+SDOF configuration the shallower location of the maximum strain transmissibility, and the different maximum values achieved (for the different sample masses) are clearly caused by the interaction between piles 4 and 5, even if the piles are not connected at the head.

It is also worth noting that the analytical value of strain transmissibility with respect to γ_1 accounting for pure kinematic interaction, computed according to [1] using a depth factor $r_d = 1$, ranges between 0.04 and 0.05 depending on the value of the frequency factor ϕ, related to the dynamic nature of the excitation:

$$\gamma_1 = \frac{r_d \rho_1 h_1 a_s}{G_1} \tag{4}$$

16

The latter theoretical value is close to the experimental one obtained in the FHP configuration. Such findings confirm that the effect of the oscillator in the FHP+SDOF configuration is able to either increase or decrease the expected response of the pile in terms of maximum strain transmissibility.
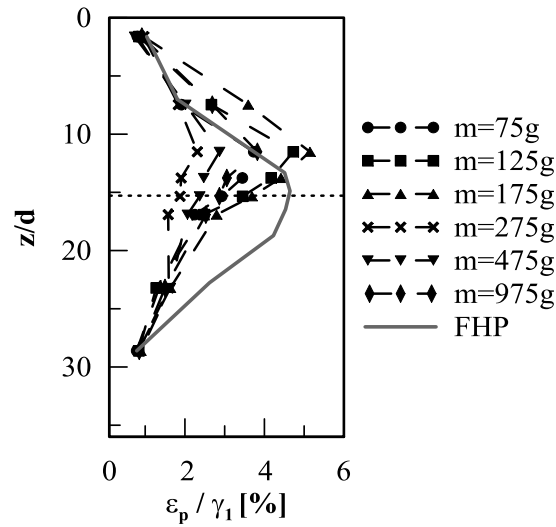

Figure 14. FHP and FHP+SDOF configurations: envelope of absolute strain transmissibility along pile 4 (sinedwell input: f=20 Hz, a_{max}=0.01g)

3.2.2. Short cap + single degree of freedom configuration

The input motion is the same as in the previous section, i.e. f=20 Hz and a=0.1g. All masses considered in the previous paragraph are here analysed, with the exception of the 75g mass that has not been tested in this configuration. The free-field responses are similar in all the tests (Figure 15a), as for the FHP+SDOF configurations. The assessment of the pile response (Figure 15b and 15c) shows that at pile heads the maximum strain transmissibility are almost similar because of the presence of the connection. These findings, i.e. the shape of the bending moment and the similar response for the two piles, were also observed in the field measurements of the Obha Ohashi Bridge and the Ervic building in Japan, as reported in [15, 2]. The envelopes of absolute strain transmissibility show a different shape along both pile 4 and 5 for the test with the mass oscillator equal to 275g; the different response is again related to the resonance condition. In fact, for this configuration the resonance occurs for a higher oscillator mass when compared to the FHP+SDOF configuration: the 275g SDOF is characterized by f = 20.5 Hz, f_s = 19.6 Hz and f_{SSI} = 19.4 Hz, that generates a very low soil-pile-structure interaction (about 5%), in agreement with the white-noise results.
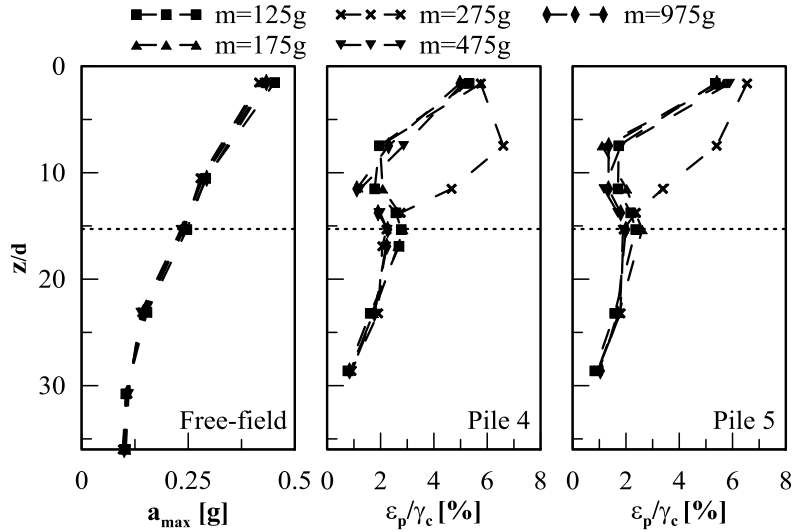
Figure 15. SC+SDOF configuration: envelope of free-field accelerations and strain transmissibility along piles 4 and pile 5 (sinedwell input: f=20 Hz, a_{max} = 0.1g)

The observation of the experimental response of the same pile-cap configuration without the oscillator (SC in Figure 4) has shown that the maximum strain transmissibilitiy at the soil layer interface is quite close to the one measured in the present tests: this evidence confirms that the inertial effects induced by the oscillator tend to vanish within the top layer. The strain transmissibility at the layer interface computed analytically using [1], is lower than those measured in these tests for both instrumented piles: such response is caused by the restrain at the pile head. It is instructive to note that the restrain at the pile head can cause either an increase or a decrease of the bending moment at the interface, depending on soil and pile geometrical and mechanical properties [48].

The maximum strain transmissibility at the heads of piles 4 and 5 for the different masses (i.e. for different resonance conditions) are reported in Figure 16a and 16b referring, respectively, to oscillator and free-field response. The increase in strain transmissibility at pile heads in resonance, already observed for the FHP+SDOF configuration (Figure 13), is present in this configuration too, although it is less significant.
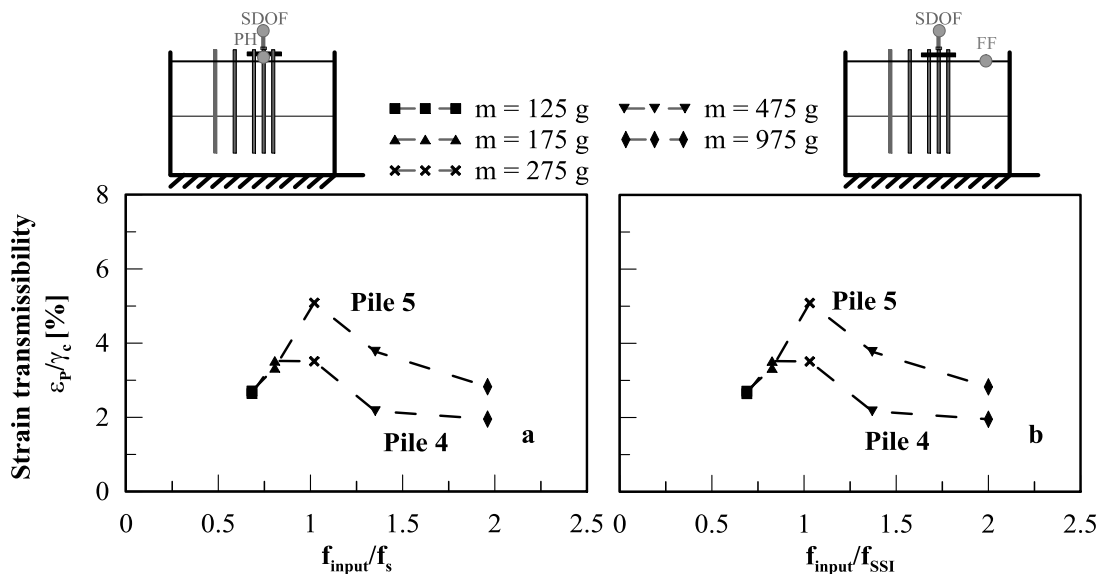

Figure 16. SC+SDOF configuration: maximum strain transmissibility at pile head versus the ratio between (a) the input and the pile head and (b) the input and the SSI frequency for piles 4 and 5 (sinedwell test: f=20 Hz, a_{max}=0.1g)

18

For this configuration, the axial forces acting on piles 4 and 5 have also been measured, using the strain-gauge recordings. In Figure 17 the forces at pile heads, expressed in a dimensionless form with reference to the oscillator self-weight (computed taking into account the weight of all the components of the physical model), are plotted versus the ratio of the input fundamental frequency and the frequency of the system, in order to investigate on the influence of the resonance condition. The lateral pile (Pile 4) response is subjected to a significant higher axial increment in resonance, due to the rocking effect induced on the cap by the oscillator. Conversely, at head of pile 5 the increment in terms of axial force is less significant, even at resonance. Hence in the SC+SDOF configuration the resonance condition causes an increment of bending moment on the central pile, whereas for the lateral pile the increment is visible in terms of the axial force.
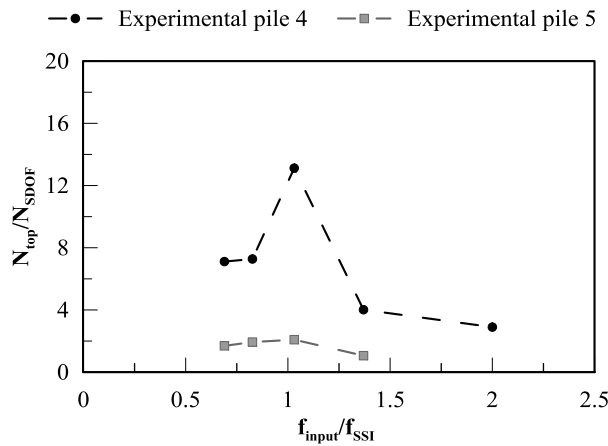

Figure 17. SC+SDOF configuration: maximum axial response at pile 4 and 5 head versus the ratio between the input and system frequencies (sinedwell test: f=20 Hz, a_{max}=0.1g)

3.2.3. Free-head pile + single degree of freedom vs short cap + single degree of freedom configuration

To further assess the effect of the configuration on pile response, the results obtained for a specific mass value are compared hereafter. The 175g mass has been chosen, as it causes resonance with the system in the FHP+SDOF configuration. The input motion is again the sinusoidal wave with 20 Hz frequency and 0.1g acceleration amplitude.

The comparison between the configuration results is shown in Figure 18: maximum soil accelerations in the free-field condition are plotted along depth; strain transmissibility curves along piles 4 and 5 are also compared in Figure 18.

The soil response in these two tests is almost the same (the classical response in free-field condition). In the FHP+SDOF configuration, the responses of the two piles are very different. Pile 5 has the maximum strain transmissibility at his head (Figure 18), because the inertial effects induced by the oscillator are not distributed among piles; then inertial effects decay rapidly inside the top layer. On the other hand, for pile 4 strain transmissibility is almost zero at the top and the bottom (because there is no oscillator attached to this pile). The maximum bending effect occurs along the pile, at a shallower depth with respect to the interface, because of the influence of the neighboring pile 5 and its superstructure. In the SC+SDOF configuration, the maximum strain transmissibility occurs at pile head for both piles 4 and 5. Because of the stiff connection at pile heads, the inertial effects are well shared by the two piles, giving strain transmissibility values quite similar for both piles; these values are obviously much lower compared to the one induced on pile 5 in the FHP configuration. The comparison also shows that, for both piles, the responses below the soil layer interface are not affected by the different configurations.
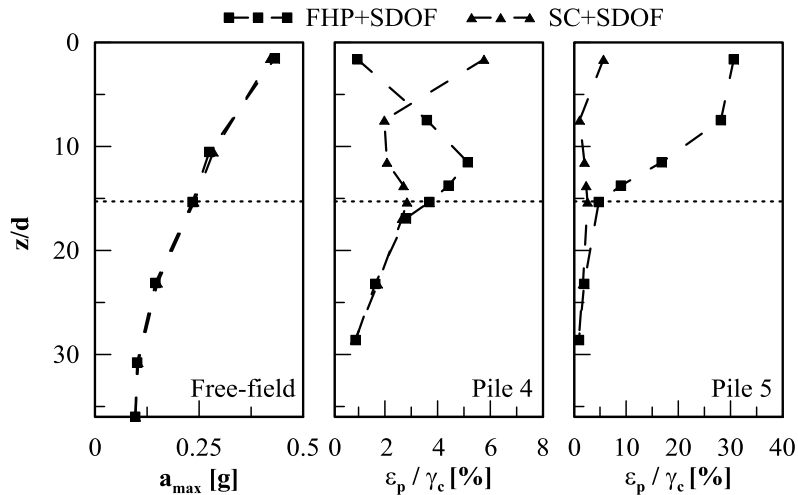
Figure 18. FHP+SDOF and SC+SDOF configurations: envelope of free-field accelerations and strain transmissibility along piles 4 and 5 (sinedwell input: f=20 Hz, a_{max} = 0.1g; m=175g)

4. Conclusions

The present paper discusses the results of a series of tests carried out at the Bristol Laboratory for Advanced Dynamics Engineering (BLADE), within the Framework of the Seismic Engineering Research Infrastructures for European Synergies (SERIES). On the 1-g shaking table apparatus different configurations of soil-pile-structure models in a bi-layered soil have been tested. In order to achieve the desired stiffness contrast between soil layers, an innovative procedure has been adopted for obtaining a higher density of the granular materials utilised (by a proper mixing of two different Leighton Buzzard sand fractions).

The present study has focused on: *(i)* the assessment of the period elongation of pile-supported systems due to SSI effects, *(ii)* the effects on pile response due to both the physical model configurations (restrain at pile heads) and *(iii)* the interaction between closely spaced piles.

As far as the period elongation is concerned, the natural frequency of the structural system has been evaluated with reference to the base of the oscillator, to the free-field surface and to the shaking table. The natural frequency relative to free-field is significantly higher than the one relative to the base of the oscillator. This finding does not comply with the fundamental (linear) SSI theory and may be attributed to nonlinear soil effects near the pile head.

The results in terms of period elongation clearly indicate that:

- for the oscillator attached to a free-head pile (FHP+SDOF configuration), the SSI interaction produces a significant increment in period (up to 20%); at prototype scale, this could be the case for slender structures, like tall bridge piers, mid-rise structures employing foundation systems supported by a limited number of piles;

- for the oscillator attached to three piles connected through a rigid cap (SC+SDOF configuration), SSI interaction produces a small increment in period (about 6%) because of the high stiffness of the connection; in fact, the stiff cap tends to reproduce the fixed base configuration. At prototype scale, this could be the case of a structure on a massive piled raft foundation.

When considering the effects of pile configurations (pile head restraint and presence of SDOF oscillator) on pile response (strain transmissibility, i.e. pile bending), interesting results have been obtained. Pile bending does not increase with oscillator mass, but it strongly depends on the degree of coupling between the frequencies of the soil-structural system (SDOF+pile+soil) and the input motion. Bending moments assume their maximum values at resonance conditions.

Main findings on pile response for the different configurations are here summarised.

• As far as the free head pile (FHP) configuration is concerned, the oscillator at the top of the

20

central pile significantly affected the response of the neighbouring pile, notwithstanding those piles are not connected at the head. This interaction produced two main effects on the neighbouring pile: i) the maximum bending location is not at the soil interface (as expected for purely kinematic interaction), but is clearly at a shallower depth; ii) the maximum bending moment varies with the mass of the oscillator on the central pile; it achieves its maximum value for the oscillator mass which induces resonance between the oscillator-pile system and the input motion.

- For the short cap configuration, inertial effects induced by the oscillator are shared between the piles connected by the stiff cap. Thus, the maximum bending effects at the pile heads are quite similar. However, they are much lower than the effects induced for the FHP configuration. At resonance, inertial actions due to the SDOF are maximum and cause different effects on the piles: (*i*) in the central pile (under the oscillator) a slight increment of the bending effects is recorded; (*ii*) on the edge piles and given the rocking of the cap, inertial actions produce significant increments in axial forces.

For all tests with oscillators attached, both on FHP and SC configurations, the results show that the inertial interaction affected the response of the pile in terms of bending moment in the upper layer (at maximum up to the layer interface), while the response of piles in the bottom layer is mainly controlled by the kinematic interaction.

In conclusion, the repeatability of the test and the significance of the obtained results indicate that the complex seismic pile-soil interaction phenomenon can be efficiently investigated by testing models on a shaking table, for an insightful understanding of their behavior leading to simple yet reliable proposals for analysis and design improvements.

References

1. Mylonakis G. Simplified model for seismic pile bending at soil layer interfaces, Soils and Foundations, 2001, 41, 47-58.
2. Nikolaou S., Mylonakis G., Gazetas G., Tazoh T. Kinematic pile bending during earthquakes: analysis and field measurements. Géotechnique; 2001, 51(5):425-440
3. Cairo R., Dente G. Kinematic interaction analysis of piles in layered soils. In 14th European Conference on Soil Mechanics and Geotechnical Engineering, ISSMGE-ERTC 12 Workshop Geotechnical Aspects of EC8, Madrid (Spain), 2007, Pàtron Editore, Bologna, cd-rom, paper n. 13

4. Padron, L.A., Aznarez, J. J., Maero, O. Dynamic analysis of piled foundations in stratified soils by a BEM-FEM model, Soil Dynamics and Earthquake Engineering, 2008, 5, 333-346.

5. Sica S, Mylonakis G, Simonelli AL. Transient kinematic pile bending in two-layer soil. Soil Dynamics and Earthquake Engineering. 2011, 31, 891-905

6. Di Laora R, Mandolini A, Mylonakis G. Insight on kinematic bending of flexible piles in layered soil. Soil Dynamics and Earthquake Engineering. 2012, 43, 309–322

7. Margason E., Halloway D.M. Pile bending during earthquakes. Proc. VI World Conference on Earthquake Engineering, Meerut, India, 1977, 1690-1696

8. Krishnan, R., Gazetas, G. and Velez, A. Static and dynamic lateral deflection of piles in non-homogeneous soil stratum, Geotechnique, 1983, 33, 307-326.

9. Kaynia, A.M., Mahzooni, S. Forces in pile foundations under seismic loading, J. Engng. Mech., ASCE, 1996, 122, 46-53.

10. Kramer SL. Geotechnical Earthquake Engineering. Prentice Hill, Upper Saddle River, NJ, USA. 1996

11. Novak, M. Piles under dynamic loads: State of the art. Proc. of 2nd International Conference on Recent Advances in Geotechnical Earthquake Engineering and Soil Dynamics, St. Louis, 1991, 3, 2433-2456

12. Gazetas G., Fan K., Tazoh T., Shimizu K., Kavvadas M., Makris N. Seismic pile-group-structure interaction. Piles under dynamic loads, Geotech. Spec. Publ. No. 34, ASCE, 1992, 56-93

13. Pender, M. Seismic pile foundation design analysis. Bulletin of the New Zealand National Society for Earthquake Engineering, 1993, 26(1), 49-160

14. Mylonakis G., Nikolaou A., Gazetas G. Soil-pile-bridge seismic interaction: kinematic and inertial effects. Part I: soft soil, Earthquake engineering and structural dynamics, 1997, 26, 337-359.

15. Gazetas, G. and Mylonakis, G. Seismic Soil-Structure Interaction: New Evidence and Emerging Issues. Geot. Earthq. Engng & Soil Dynamics III, Geo-Institute ASCE Conference, Seattle, 1998, P. Dakoulas, M.K. Yegian, & R.D. Holtz (eds), Vol. II, 1119-1174

16. Chau, K.T., Shen, C.Y. and Guo, X. Non-linear seismic soil-pile-structure interaction: Shaking table tests and FEM analyses, Soil Dynamics and Earthquake Engineering, 2009, 29, 300-310;

17. Eurocode 8. Design of structures for earthquake resistance, Part 5: Foundations, retaining structures and geotechnical aspects, CEN E.C. for Standardization, Bruxelles, 2004

18. Federal Emergency Management Agency. Prestandard and Commentary for the Seismic Rehabilitation of Buildings, FEMA Document No. 356, 2000, Washington D.C., USA

19. Federal Emergency Management Agency. Improvement of Nonlinear static analysis procedures, FEMA Document No. 440, 2005, Washington, D.C. USA

20. NIST. Soil-structure interaction for building structures. National Institute of Standards and Technology, U.S. Department of Commerce, Washington D.C. Project Technical Committee: Stewart, JP (Chair), CB Crouse, T Hutchinson, B Lizundia, F Naeim, and F Ostadan. 2012, Report No. NIST GCR 12-917-21;

21. Dezi F, Carbonari S, Leoni G. Kinematic bending moments in pile foundations. Soil Dynamics and Earthquake Engineering. 2009, 30(3):119–132

22. Meymand P. J. (1998). Shaking Table Scale Model Tests of Nonlinear Soil-Pile-Superstructure Interaction In Soft Clay. PhD Thesis, University of California, Berkeley

23. Muir Wood D., Crewe A. and Taylor C. A. (2002). Shaking table testing of geotechnical models. IJPMG - International Journal of Physical Modelling in Geotechnics 1, 2002, 01-13

24. Pitilakis D, Dietz M, Wood DM, Clouteau D, Modaressi A. Numerical simulation of dynamic soil–structure interaction in shaking table testing. Soil Dynamics and Earthquake Engineering. 2008, 28, 453–467

25. Dihoru, L., Bhattacharya, S., Taylor, C.A, Muir Wood, D. Moccia, F., Simonelli. A.L. and Mylonakis, G. Experimental modeling of kinematic bending moments of piles in layered soils, IS-Tokyo, 2009

26. Dihoru, L., Bhattacharya, S., Taylor, C.A, Muir Wood, D. Moccia, F., Simonelli. A.L. and Mylonakis, G. Physical and Numerical Modelling of kinematic pile-soil interaction under seismic conditions, Physical Modelling Conference, Zurich 2010

27. Simonelli, A.L., Di Sarno, L., Durante, M.G., Sica, S., Bhattacharya, Dietz, M., Dihoru, L., Taylor, C.A., Cairo, R., Chidichimo, A., Dente, G., Anoyatis, G., Mylonakis, G., Modaressi, A., Todo Bom, L. and Kaynia, A.M. Experimental Assessment of Soil-Pile-Structure Seismic Interaction – Chapter 26. in Seismic Evaluation and Rehabilitation of Structures, Edited by Ilki, A. and Fardis, M. Editor, Geotechnical, Geological and Earthquake Engineering Series, Springer, 2014, ISBN 978-3-319-00457-0

28. Chidichimo A. Experimental and analytical investigation on soil-pile-structure interaction PhD Thesis, Università "Mediterranea" Reggio Calabria, 2014

29. Durante M. G. Experimental and numerical assessment of dynamic soil-pile-structure interaction. Ph.D. Thesis, Universita' degli Studi di Napoli Federico II, Napoli, 2015

30. Crewe A.J., Lings, M.L., Taylor, C.A., Yeung, A.K. & Andrighetto. Development of a large flexible shear stack for testing dry sand and simple direct foundations on a shaking table' European seismic design practice, Elnashai (ed), Balkema, Rotterdam, 1995

31. Stroud, M. A. The behaviour of sand at low stress levels in the simple shear apparatus. PhD thesis, University of Cambridge, 1971

32. Tan FSC. Centrifuge and theoretical modelling of conical footings on sand. PhD Thesis, University of Cambridge, 1990

33. Cavallaro, A., Maugeri, M. & Mazzarella, R. Static and dynamic properties of Leighton Buzzard sand from laboratory tests. 4th International Conference on Recent Advances in Geotechnical Earthquake Engineering and Soil Dynamics, San Diego, CA, 2001, Paper 1.13

34. Lings, M.L., Dietz, M.S. An improved direct shear apparatus for sand. Geotechnique, 2004, 54: 4, 245–256

35. Moccia F. Seismic soil pile interaction: experimental evidence. Ph.D. Thesis, Universita' degli Studi di Napoli Federico II, Napoli, 2009

36. Durante M. G., Karamitros D., Di Sarno L., Sica S., Taylor C. A., Mylonakis G., Simonelli A. L. Characterisation of shear wave velocity profiles of non-uniform bi-layer soil deposits: analytical evaluation and experimental validation. Soil Dynamics and Earthquake Engineering. 2015, 75: 44-54

37. CSI Analysis Reference Manual for SAP2000, ETABS and SAFE. Computers and Structures, Inc., Berkeley, CA, USA. 2013

38. Veletsos, A. S. Dynamics of Structure-Foundation Systems, in: Hall, W. J. (ed.), Structural & Geotechnical Mech., Prentice-Hall, 1977

39. Ciampoli M and Pinto PE. Effects of soils-structure interaction on inelastic seismic response of bridge piers. Journal of Structural Engineering, ASCE. 1995, 121(5), 806-814.

40. Stewart JP, Fenves GL and Seed RB. Seismic soil-structure interaction in buildings. I: Analytical methods. J Geotech & Geoenv Engrg, ASCE. 1999, 125(1), 26-37;

41. Kumar S, Prakash S. Estimation of fundamental period for structures supported on pile foundations. Geotech Geol Eng 2004; 22: 375–89

42. Maravas A., Mylonakis G., Karabalis D. L.. Simplified discrete systems for dynamic analysis of structures on footings and piles. Soil Dynamics and Earthquake Engineering. 2014, 61-62: 29-39

43. Jennings PC, Bielak J. Dynamics of building–soil interaction. Bull SeismolSoc Am 1973;63(1):9–48

44. Veletsos AS,Nair VVD. Seismic interaction of structures on hysteretic foundations. J StructDiv 1975; 101(1): 109–29

45. Wolf J P. Soil–structure interaction. New Jersey, USA: Prentice Hall; 1985

46. Durante MG, Di Sarno L, Sica S, Mylonakis G, Taylor CA, Simonelli AL. Experimental measurements of geotechnical system in 1-g tests. Proc. of 20th IMEKO TC4 Symposium on Measurements of Electrical Quantities: Research on Electrical and Electronic Measurement for the Economic Upturn, Benevento – Special Session: Advanced Measurements in Geotechnics, 2014

47. Chidichimo A, Cairo R, Dente G, Taylor C, Mylonakis G. 1-g experimental investigation of bi-layer soil response and kinematic pile bending. Soil Dynamics and Earthquake Engineering 2014; 67:219–232.

48. Di Laora R, Mylonakis G, Mandolini A. Pile-head kinematic bending in layered soil. Earthquake Engineering and Structural Dynamics 2013; 42:319–337.